THE JOURNAL OF PHYSICAL CHEMISTRY B

Article

pubs.acs.org/JPCB

Photoactive Fluoropolymer Surfaces That Release Sensitizer Drug Molecules

Goutam Ghosh,[†] Mihaela Minnis,[†] Ashwini A. Ghogare,[†] Inna Abramova,[†] Keith A. Cengel,[‡] Theresa M. Busch,[‡] and Alexander Greer*[,†]

[†]Department of Chemistry and Graduate Center, Brooklyn College, City University of New York, Brooklyn, New York 11210, United States

[‡]Department of Radiation Oncology, University of Pennsylvania, Philadelphia, Pennsylvania 19104, United States

Supporting Information

ABSTRACT: We describe a physical−organic study of two fluoropolymers bearing a photoreleasable PEGylated photosensitizer that generates $^1O_2(^1\Delta_g)$ [chlorin e_6 methoxy tri(ethylene glycol) triester]. The surfaces are Teflon/poly(vinyl alcohol) (PVA) nanocomposite and fluorinated silica. The relative efficiency of these surfaces to photorelease the PEGylated sensitizer [shown previously to be phototoxic to ovarian cancer cells (Kimani, S. et al. *J. Org. Chem* **2012**, *77*, 10638)] was slightly higher for the nanocomposite. In the presence of red light and O_2, $^1O_2$ is formed, which cleaves an ethene linkage to liberate the sensitizer in 68−92% yield. The fluoropolymers were designed to deal with multiple problems. Namely, their success relied not only on high O_2 solubility and drug repellency but also on the C−F bonds, which physically quench little $^1O_2$, for singlet oxygen's productive use away from the surface. The results obtained here indicate that Teflon-like surfaces have potential uses in delivering sensitizer and singlet oxygen for applications in tissue repair and photodynamic therapy (PDT).

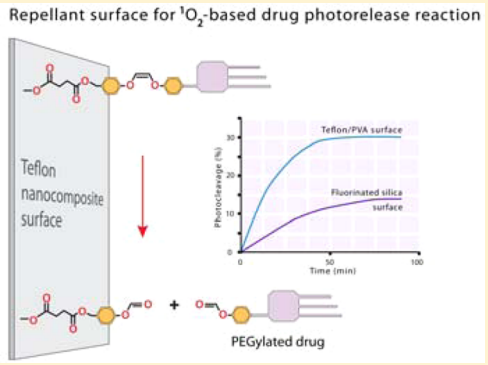

INTRODUCTION

Solid supports have been used as platforms for the photorelease of drug molecules.[1,2] However, there are gaps in data on whether Teflon-like[3,4] or superhydrophobic surfaces[5] can efficiently photorelease drugs. To address this issue, two photoactive fluoropolymers have been synthesized and compared (Figure 1). One is made of fluorinated silica [glass coated with $(CH_3O)_3SiCH_2CH_2CF_2CF_2CF_2CF_3$], and the other is a Teflon/poly(vinyl alcohol) (PVA) nanocomposite that has $-[CF_2-CF_2]_m-$ and $-[CH_2-CH(OH)]_n-$ chains. Figure 1 also shows that the sensitizer drug to be photoreleased is PEGylated.

While the delivery of PEGylated compounds is an active area of research,[6−8] they tend to adhere to surfaces.[9−11] Even though solid-state sensitizers have been established,[12−14] few have been designed to release PEGylated compounds,[15] and none have capitalized on fluoropolymers' nonstick repellent properties[16] for better molecule discharge from the surface. Thus, we anticipated that fluoropolymer sensitizer release systems with repellent properties and visible light activation could be established.

Visible light and NIR photocleavage reactions are known[17−24] and actually represent a burgeoning area of research.[25,26] For example, the sensitized generation of $^1O_2(^1\Delta_g)$ has been used with labile ethene linkers for photorelease reactions. We[27,28] and others[29−31] have published papers devoted to $^1O_2$-based drug release, and a book chapter has also appeared.[32] Singlet oxygen is a potentially therapeutic species and is photogenerated by PAHs,[33,34] chlorins,[35,36] porphyrins and phthalocyanines, and their fluorinated analogues.[37−41] In 2011, Röder et al. reported the deposition of perfluorinated phthalocyanines on silica gel as a composite material for generating $^1O_2$ for sterilization.[42] A Teflon ponytail fullerene (i.e., C_{60} adduct with $CH_2[CO_2(CH_2)_3(CF_2)_7CF_3]_2$) has also been prepared for $^1O_2$ generation.[43] Favorable properties of surface fluorination for $^1O_2$ and drug potency through PEGylation would make such a combination be desirable. However, solid materials that are both fluorinated and PEGylated are rather uncommon.[44] Taken together, the above topics reveal the potential utility of a Teflon-supported PEGylated drug release system and point to the need for new studies.

Our hypothesis was that a Teflon/PVA nanocomposite will photorelease the PEGylated sensitizer more efficiently than fluorinated silica because of the higher number of C−F bonds in the former. Thus, we report here the synthesis and study of two fluoropolymers illustrated in Figure 1 to give us insight into the photosensitizer release mechanism. We show that these surfaces have (i) high solubility of ground-state oxygen, which is advantageous for photooxidation chemistry; (ii) relatively low adsorptivity for the PEGylated sensitizer, for good turnout; (iii) facile breakage of the ethene linker bond; and (iv) longer singlet

Received: January 26, 2015
Revised: February 13, 2015
Published: February 16, 2015

DOI: 10.1021/acs.jpcb.5b00808
J. Phys. Chem. B 2015, 119, 4155−4164

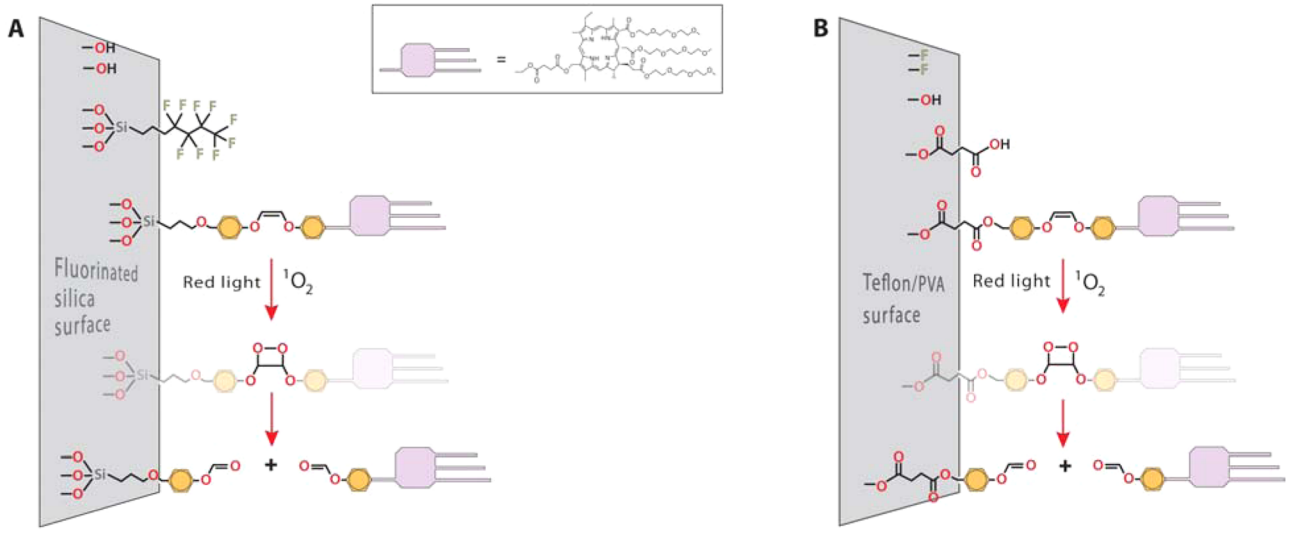

Figure 1. Design of fluoropolymer surfaces tailored for $^1O_2$-initiated sensitizer drug photorelease reactions. The sensitizer, a chlorin derivative PEGylated with triethylene glycol, was bound to surface OH groups of (A) fluorinated silica (Vycor glass monolith coated with nonafluorosilane) and (B) a Teflon/poly(vinyl alcohol) nanocomposite. Red light irradiation leads to the reaction of $^1O_2$ with the ethene, resulting in the formation of a dioxetane. A second step follows with cleavage to release the sensitizer.

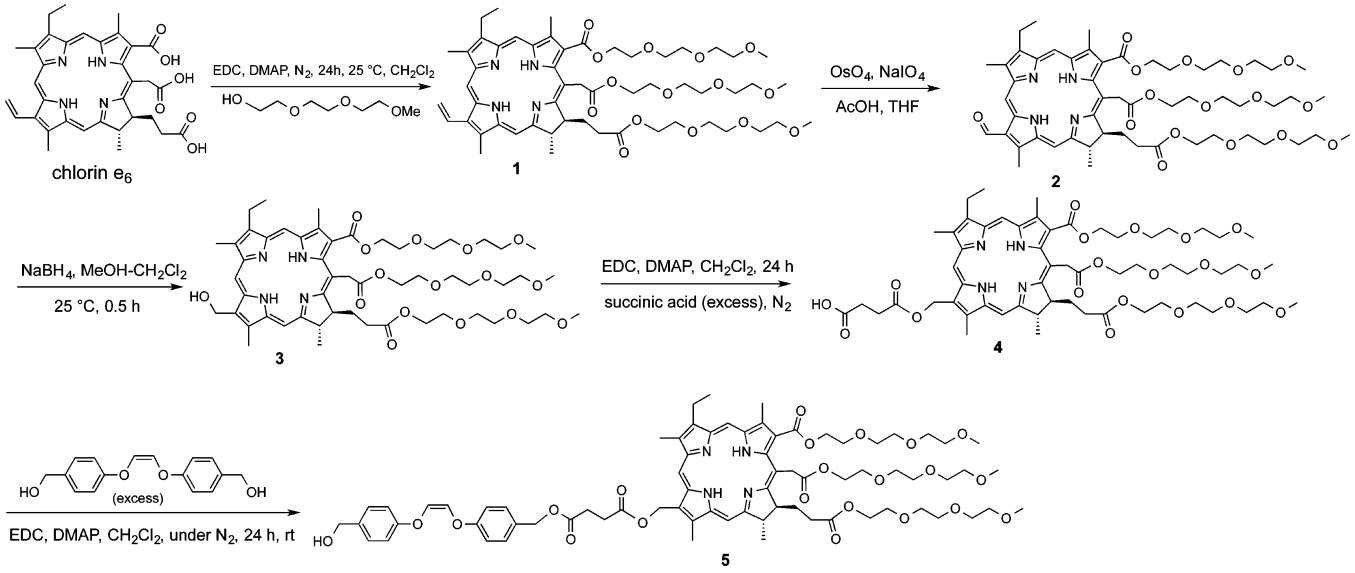

Figure 2. Synthesis of spacer triPEG chlorin **5**.

oxygen lifetimes (τ_Δ) because the C−F bonds sap the polymer's ability to physically quench $^1O_2$ (i.e., the paucity of C−H and O−H bonds limits unwanted vibrational relaxation of $^1O_2$ to $^3O_2$). The fluoropolymers we describe are biocompatible (e.g., for surgery),[45,46] and our mechanistic study provides results that may be useful for applications in localized delivery of sensitizer to desired surfaces (e.g., wounds or diseased tissue), where the released photosensitizer is active upon subsequent illumination.

EXPERIMENTAL SECTION

General Aspects. Reagent grade solvents methanol, hexane, toluene, DMF, THF, CH_2Cl_2, $CHCl_3$, $CDCl_3$, CCl_4, and *n*-butanol were used. Hydrofluoric acid, sodium sulfate, sodium bicarbonate, sodium periodate, sodium borohydride, osmium tetroxide, acetic acid, succinic acid, *N*-(3-(dimethylamino)-propyl)-*N*′-ethylcarbodiimide hydrochloride (EDC), *N*,*N*-dimethyl-4-aminopyridine (DMAP), (3-iodopropyl)-trimethoxysilane, 3,3,4,4,5,5,6,6,6-nonafluorohexyltrimethoxysilane, tri(ethylene glycol) monomethyl ether, chlorin e_6, rose bengal, poly(vinyl alcohol) (MW 89 000−98 000, and 99% hydrolyzed), and poly(tetrafluoroethylene) (PTFE: 60 wt % solid content, 5.9 wt % nonionic surfactant, 22.3 nm average particle size, and 2.20 g/mL density) were used as received from commercial suppliers. Solid samples were cleaned with refluxing methanol in a Soxhlet extractor. Proton and carbon NMR data were recorded at 400 and 100.6 MHz, respectively. UV−vis and IR spectrophotometers, a GC/MS instrument, a muffle furnace, and a portable pO_2 oxygen sensor were also used. HRMS data were collected at the mass spectrometry facility in University of California, Riverside.

Synthesis of 3-Formyl-17^3,15^2,13^1-chlorin e_6 Methoxy Tri(ethylene glycol) Triester (2) (Figure 2). Yield, 12.0 mg (60%); purity, 98%. Chlorin e_6 was converted to triPEG chlorin **1** (i.e., methoxy triethylene glycol attached at the ester bonds for a

DOI: 10.1021/acs.jpcb.5b00808
J. Phys. Chem. B 2015, 119, 4155−4164

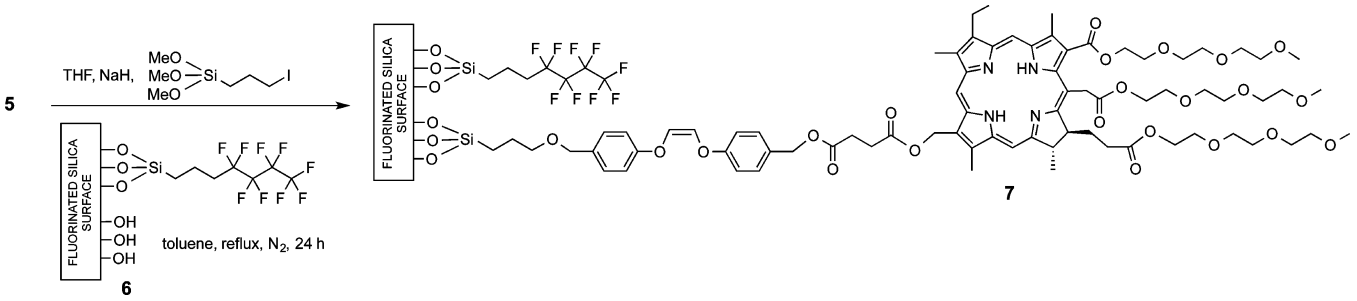

Figure 3. Synthesis of sensitizer conjugated organically to fluorinated silica **7**.

3:1 conjugate) by a previously described procedure.[47] To 20.0 mg (0.019 mmol) of **1** in 15 mL THF was added 7.68 mg (0.03 mmol) of OsO_4 in 20 μL CCl_4 at 0 °C under a N_2 atmosphere. Reaction mixture was stirred under 0−5 °C temperature for 25 min. 82.8 mg (0.38 mmol) of $NaIO_4$ was dissolved in 1% AcOH solution and added to the reaction mixture. Reaction was stirred overnight at room temperature. A drop of saturated sodium bicarbonate solution was added to neutralize the acid. The reaction mixture was extracted with 50 mL of CH_2Cl_2 and washed with water. The organic layer was dried over sodium sulfate. After evaporating the organic solvent, the residue was purified by column chromatography using 1.1% methanol−CH_2Cl_2. R_f = 0.69 in 3% methanol−CH_2Cl_2. HPLC: t_R = 12.2 min in a gradient mixture of methanol and H_2O. ^{1}H NMR (400.0 MHz, $CDCl_3$) δ 11.56 (s, 1H), 10.28 (s, 1H), 9.70 (s, 1H), 8.97 (s, 1H), 5.48 (d, J = 18.4 Hz, 1H), 5.30 (d, J = 18.4 Hz, 1H), 4.96 (m, 1H), 4.89 (m, 1H), 4.51 (m, 2H), 4.35 (m, 2H), 4.16 (m, 4H), 3.86 (m, 3H), 3.84 (s, 3H), 3.82 (m, 3H), 3.71 (t, J = 4.8 Hz, 3H), 3.65 (m, 5H), 3.56 (m, 10H), 3.44 (t, J = 4.8 Hz, 3H), 3.37 (s, 3H), 3.34 (m, 4H), 3.30 (s, 3H), 3.23 (s, 3H), 3.22 (s, 3H), 3.18 (t, J = 4.8 Hz, 2H), 2.60 (m, 1H), 2.25 (m, 2H), 1.77 (m, 8H), −1.24 (br s, 1H), 1.76 (br s, 1H). ^{13}C NMR (100.6 MHz, $CDCl_3$) δ 188.3, 173.0, 172.2, 168.9, 168.5, 167.6, 155.1, 151.5, 144.9, 138.3, 138.1, 137.9, 136.6, 136.0, 134.0, 131.9, 128.6, 125.8, 103.4, 101.3, 100.7, 95.5, 71.9, 71.8, 71.6, 70.7, 70.6, 70.5, 70.4, 70.2, 70.1, 69.2, 69.0, 68.9, 65.2, 64.3, 63.6, 59.0, 58.9, 58.8, 53.4, 48.7, 38.5, 31.0, 29.7, 29.5, 23.3, 19.6, 17.5, 12.4, 11.4, 11.3. HRMS (+ESI) m/z calcd for $C_{54}H_{77}N_4O_{16}$ $[M + H]^+$, 1037.5335; found, 1037.5357. UV−vis ($CHCl_3$) λ_{max} 418 and 694 nm.

Synthesis of 3^1-Hydroxyl-17^3,15^2,13^1-chlorin e$_6$ Methoxy Tri(ethylene glycol) Triester (3). Yield, 10.0 mg (77%); purity, 92%. To 13.0 mg (0.012 mmol) of **2** in 4:1 mL methanol−CH_2Cl_2 at 5−10 °C was added 1.0 mg (0.025 mmol) of $NaBH_4$. A sudden color change from brown to green was observed. The reaction was monitored by TLC. It was completed in 0.5 h. The reaction mixture was quenched with water and extracted by CH_2Cl_2. The organic layer was dried over sodium sulfate and evaporated by a rotavapor system. R_f = 0.50 in 3% methanol−CH_2Cl_2. HPLC: t_R = 7.79 min in a gradient mixture of methanol and H_2O. ^{1}H NMR (400.0 MHz, $CDCl_3$) δ 9.72 (s, 1H), 9.55 (s, 1H), 8.76 (s, 1H), 5.87 (s, 2H), 5.44 (d, J = 18.8 Hz, 1H), 5.29 (d, J = 19.6 Hz, 1H), 4.93 (m, 1H), 4.88 (m, 1H), 4.47 (m, 2H), 4.32 (m, 2H), 4.11 (m, 4H), 3.85 (m, 3H), 3.79 (m, 3H), 3.70 (t, J = 4.8 Hz, 2H), 3.60 (m, 5H), 3.55 (t, J = 4.8 Hz, 3H), 3.48 (m, 11H), 3.40 (m, 2H), 3.36 (s, 3H), 3.30 (s, 3H), 3.28 (s, 3H), 3.20 (m, 4H), 3.16 (m, 3H), 3.11 (m, 2H), 3.02 (t, J = 4.8 Hz, 2H), 2.27 (m, 1H), 2.16 (m, 1H), 2.09 (m, 2H), 1.86 (m, 2H), 1.75 (m, 7H), −1.58 (br s, 1H). ^{13}C NMR (100.6 MHz, $CDCl_3$) δ 173.0, 172.4, 169.7, 168.8, 166.8, 154.5, 148.9, 145.0, 139.1, 136.6, 136.0, 135.7, 135.5, 135.2, 132.5, 129.4, 123.7, 102.6, 102.0, 98.2, 93.7, 71.9, 71.7, 71.5, 70.7, 70.6, 70.3, 70.1, 70.0, 69.2, 68.8, 65.0, 64.3, 63.5, 59.0, 58.9, 58.7, 56.3, 53.4, 52.9, 49.3, 38.6, 30.9, 29.7, 29.6, 23.0, 19.6, 17.6, 14.1, 12.4, 11.3, 11.1. HRMS (+ESI) m/z calcd for $C_{54}H_{79}N_4O_{16}$ $[M + H]^+$, 1039.5491; found, 1039.5490. UV−vis ($CHCl_3$) λ_{max} 404 and 661 nm.

Synthesis of 3^1-Succinate-17^3,15^2,13^1-chlorin e$_6$ Methoxy Tri(ethylene glycol) Triester (4). Yield, 8.0 mg (73.4%); purity, 90%. To 10.0 mg (0.0096 mmol) of **3** in 10 mL of dry CH_2Cl_2 under a N_2 atmosphere were added 5.65 mg (0.048 mmol) of succinic acid, 4.57 mg (0.024 mmol) of EDC, and 2.9 mg (0.024 mmol) of DMAP. Reaction was stirred for 36 h under N_2 at room temperature, after which 15 mL of CH_2Cl_2 was added. The organic layer was washed with water and dried over sodium sulfate. The organic layer was evaporated, and **3** was purified by 2% methanol−CH_2Cl_2. R_f = 0.37 in 3% methanol−CH_2Cl_2. HPLC: t_R = 7.79 min in a gradient mixture of methanol and H_2O. ^{1}H NMR (400.0 MHz, $CDCl_3$) δ 9.73 (s, 1H), 9.58 (s, 1H), 8.80 (s, 1H), 6.46 (s, 2H), 5.44 (d, J = 18.4 Hz, 1H), 5.29 (d, J = 19.6 Hz, 1H), 4.92 (m, 2H), 4.48 (m, 2H), 4.30 (t, J = 4.8 Hz, 2H), 3.80 (m, 6H), 3.70 (t, J = 4.8 Hz, 2H), 3.62 (s, 3H), 3.55 (m, 4H), 3.51 (s, 3H), 3.47 (s, 3H), 3.45 (m, 4H), 3.36 (m, 8H), 3.23 (s, 3H), 3.11 (s, 3H), 3.07 (m, 2H), 2.99 (t, J = 4.8 Hz, 2H), 2.88 (m, 2H), 2.82 (m, 2H), 2.75 (m, 2H), 2.69 (m, 2H), 2.48 (m, 2H), 2.29 (m, 4H), 1.86 (m, 2H), 1.74 (dd, J = 16.4 Hz, 11.6 Hz, 6H), −1.67 (br s, 1H). HRMS (+ESI) m/z calcd for $C_{58}H_{83}N_4O_{19}$ $[M + H]^+$, 1139.5652; found, 1139.5634.

Synthesis of Spacer Alkene-3^1-Succinate-17^3,15^2,13^1-chlorin e$_6$ Methoxy Tri(ethylene glycol) Triester (5). Yield, 1.9 mg (52%); purity, 91%. To 3.0 mg (0.0026 mmol) of **4** in dry CH_2Cl_2 under a N_2 atmosphere were added 2.0 mg (0.0073 mmol) of spacer alkene alcohol, 1.06 mg (0.0052 mmol) of EDC, and 1.0 mg (0.0078 mmol) of DMAP. Reaction was stirred for 36 h under N_2 at room temperature, after which 15 mL of CH_2Cl_2 was added. Organic layer was washed with water and dried over sodium sulfate. The organic layer was evaporated, and **5** was purified by 1.5% methanol−CH_2Cl_2. R_f = 0.64 in 3% methanol−CH_2Cl_2. HPLC: t_R = 9.24 min in a gradient mixture of methanol and H_2O. ^{1}H NMR (400.0 MHz, $CDCl_3$) δ 9.73 (s, 1H), 9.58 (s, 1H), 8.80 (s, 1H), 7.32 (d, J = 8.4 Hz, 2H), 7.01 (d, J = 8.4 Hz, 2H), 6.97 (d, J = 8.4 Hz, 2H), 6.71 (d, J = 8.4 Hz, 2H), 6.45 (s, 2H), 5.91 (d, J = 3.2 Hz, 1H), 5.71 (d, J = 3.2 Hz, 1H), 5.44 (d, J = 18.8 Hz, 1H), 5.27 (d, J = 18.4 Hz, 1H), 4.89 (m, 4H), 4.61 (s, 2H), 4.47 (m, 2H), 4.33 (m, 2H), 4.14 (m, 5H), 3.83 (m, 3H), 3.77 (m, 3H), 3.70 (t, J = 4.8, 4H), 3.62 (m, 5H), 3.56 (m, 10H), 3.50 (s, 3H), 3.43 (m, 3H), 3.36 (s, 3H), 3.33 (s, 3H), 3.29 (s, 3H), 3.21 (m, 7H), 3.14 (t, J = 4.8 Hz, 2H), 2.80 (m, 2H), 2.74 (m, 2H), 2.55 (m, 1H), 2.19 (m, 3H), 1.73 (m, 7H), −1.40 (br s, 1H), −1.65 (br s, 1H). ^{13}C NMR (100.6 MHz, $CDCl_3$) δ 173.5,

DOI: 10.1021/acs.jpcb.5b00808
J. Phys. Chem. B 2015, 119, 4155−4164

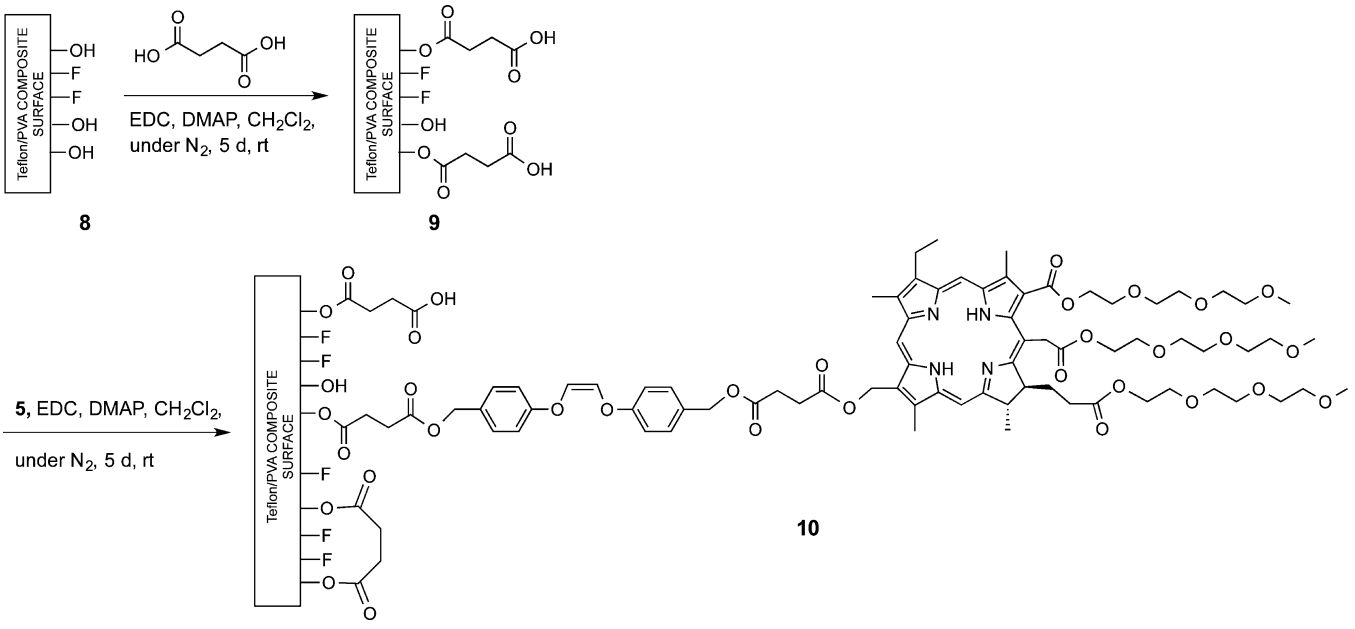

Figure 4. Synthesis of sensitizer conjugated organically to Teflon/PVA nanocomposite **10** and byproduct formation of surface diester sites.

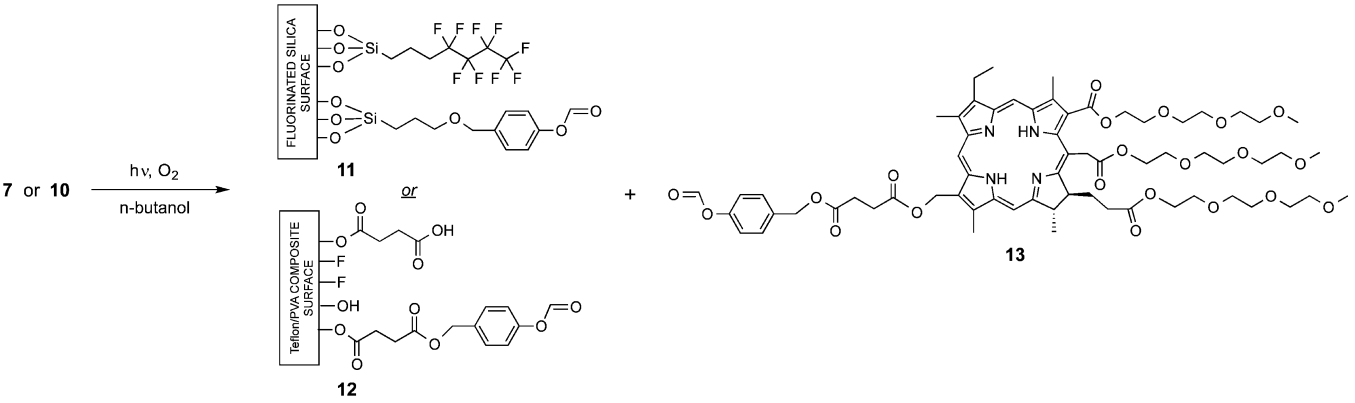

Figure 5. Photooxidation of fluorinated silica **7** and Teflon/PVA nanocomposite **10** leads to the photorelease of sensitizer **13**.

173.0, 172.4, 172.2, 172.0, 169.5, 168.7, 167.1, 157.0, 156.7, 145.0, 138.6, 136.7, 136.2, 135.6, 135.5, 135.2, 134.0, 130.7, 129.8, 129.7, 129.6, 128.4, 127.6, 123.9, 116.1, 115.8, 101.9, 98.3, 94.0, 71.9, 71.8, 71.5, 70.7, 70.6, 70.5, 70.4, 70.1, 69.2, 68.9, 66.8, 66.0, 65.0, 64.7, 64.3, 63.5, 59.0, 58.9, 58.8, 57.6, 53.4, 53.0, 49.2, 38.7, 38.6, 34.0, 31.0, 30.4, 29.7, 29.6, 29.3, 29.2, 28.9, 24.4, 23.8, 23.0, 22.9, 19.6, 17.7, 14.1, 14.0, 12.4, 11.3, 11.0. HRMS (+ESI) m/z calcd for $C_{74}H_{97}N_4O_{22}$ $[M + H]^+$, 1393.6594; found, 1393.6592. UV−vis ($CHCl_3$) λ_{max} ($\varepsilon/M^{-1}cm^{-1}$) 400 nm (338 680), 661 nm (92 760).

TriPEG Chlorin-Modified Fluorinated Silica (7) (Figure 3). Fluorinated glass **6** was prepared based on the methods established from our previous work.[48] Briefly, Vycor pieces were added to the nonafluorotrimethoxysilane in 0.07 wt % in toluene and refluxed for 24 h under N_2. Unreacted nonafluorotrimethoxysilane was washed off of the silica by Soxhlet extraction in methanol for 24 h. TriPEG chlorin **5** reacted with (3-iodopropyl)trimethoxysilane and was added to twelve pieces of fluorinated silica **6** [each piece was 0.33 g and sized ~5 mm × ~8 mm ($d \times l$)] in refluxing toluene for 24 h to reach **7**. Washing with CH_2Cl_2, THF, methanol, and hexane was followed by a Soxhlet extraction in methanol for 24 h to remove any adsorbed sensitizer from the silica. No sensitizer leaching from the surface was observed in the dark or under subdued light. UV−vis (λ_{max}, air) 400 and 661 nm. After dissolution of silica **7** by HF treatment and extraction with $CHCl_3$, evidence suggested the liberation of sensitizer (Soret band observed at 400 nm): $HOCH_2C_6H_4O$-$CH{=}CHOC_6H_4CH_2OCH_2CH_2CH_2SiF_3$ (+ESI) m/z calcd for $C_{19}SiH_{20}O_4F_3$, 398; found, 399, and $HOCH_2C_6H_4OCH{=}CHOC_6H_4CH_2OCH_2CH_2CH_2Si(OH)_3$ (+ESI) m/z calcd for $C_{19}H_{24}O_7Si$, 392; found, 391. The amount of sensitizer that was loaded into **7** was 90 nmol/g of silica.

TriPEG Chlorin-Modified Teflon/PVA (10) (Figure 4). Teflon/PVA **8** was prepared from a literature procedure and is a polymeric nanocomposite material of a PVA matrix filled with Teflon nanospheres.[49] Teflon suspension was added to a PVA solution (PVA dissolved in boiling H_2O with stirring for 5 h) in a 6:1 Teflon/PVA mass ratio. The mixture was stirred at room temperature and atmospheric pressure for 2.5 h using a mechanical agitator. Samples were placed in a mold and dried at room temperature and atmospheric pressure for 1 week. FT-IR (cm^{-1}): 3600−3100, 2950−2850, 1419−1325, 1203, 1147. UV−vis (λ, air): transparent. Succinic acid (0.100 g, 8.5 mmol) was dissolved in 1 mL of anhydrous DMF and added to five pieces (ea. 0.22 g) of Teflon/PVA in 15 mL of anhydrous CH_2Cl_2. EDC (0.081 g, 0.425 mmol) and DMAP (0.052 g, 0.425 mmol) were

DOI: 10.1021/acs.jpcb.5b00808
J. Phys. Chem. B 2015, 119, 4155−4164

added, and the mixture was stirred under a N_2 atmosphere for 5 days. The samples were washed with CH_2Cl_2, THF, methanol, toluene, and hexane and then Soxhlet extracted with methanol for 24 h to reach Teflon/PVA **9**. FT-IR (cm^{-1}): 1723. UV−vis (λ, air): transparent. TriPEG chlorin **5** (6 mg, 4.3 μmol), EDC (0.010 g, 0.052 mmol), and DMAP (0.010 g, 0.082 mmol) were added to five pieces of Teflon/PVA **9** [each piece was 0.21 g and sized ~4 mm × ~7 mm ($d \times l$)] in 10 mL of CH_2Cl_2 under a N_2 atmosphere. The reaction mixture was stirred for 5 days. After completion of the reaction, the samples were washed with several solvents (CH_2Cl_2, THF, methanol, toluene, hexane) and Soxhlet extracted using methanol for 24 h. FT-IR (cm^{-1}): 1731. UV−vis (λ, air): 396 and 660 nm. The amount of sensitizer attached onto the succinic acid sites of Teflon/PVA was determined to be 23.4 nmol/g by UV−vis spectroscopy. IR data were unable to distinguish whether the excess EDC used converted many of the surface acid sites to diesters (Figure S22, Supporting Information). Teflon/PVA **10** was stable in the dark; the sensitizer did not leach out to any measurable extent after CH_2Cl_2, methanol, THF, and hexane solvent washings or Soxhlet extraction with methanol.

Photorelease of Sensitizer 13 from Surfaces 7 and 10 (Figure 5). The photolysis setup included a continuous wave diode laser (669 nm output) where the light was passed through an SMA port and out of the end of a borosilicate optical fiber with SMA optical fiber coupling, as has been described in our previous work.[48] Under subdued light, *n*-butanol solutions were presaturated with O_2 for 20 min and then illuminated with red light for 1.5 h, upon which $^1O_2$ was generated and trapped by the alkene sites on the solid supports. These heterogeneous photolysis reactions contained 0.328 and 0.214 g of solids **7** and **10**, respectively. Concentrations of **13** were measured based on calibration curves, which followed its Q-band absorption at 665 nm. The number of broken alkene bond was quantified by the amount of sensitizer detected in after Soxhlet extraction in methanol. Control experiments demonstrated that the photorelease does not deviate from Beer's law in the UV−vis detection of sensitizer. Compound **13**: HRMS (+ESI) m/z calcd for $C_{66}H_{89}N_4O_{21}$ $[M + H]^+$, 1273.6014; found, 1273.6018. UV−vis ($CHCl_3$) λ_{max} 399 and 660 nm. No other products were found in solution based on GC/MS and NMR spectroscopy.

Lifetime Measurements. The singlet oxygen lifetime was determined using the output of a Continuum Surelite I-20 Nd:YAG pumped Surelite OPO Plus (type I BBO broadband) laser producing 5 ns pulses of 460 nm light at ~0.2 mJ/pulse and a Hamamatsu H10330B-45 photomultiplier tube at an operating voltage of 650 V. Four-milliliter O_2-saturated solutions of acetone-h_6 were used containing 2.5×10^{-4} M rose bengal and 75−150 μm sized silica and ~300−400 μm sized Teflon particles. The $^1O_2$ luminescence intensity was monitored at a right angle through an interference filter centered at 1270 nm. The $^1O_2$ signal was recorded on a 600 MHz oscilloscope (LeCroy WaveSurfer) and processed with OriginPro software.

RESULTS AND DISCUSSION

O_2 Solubility Enhancements (Table 1). Table 1 shows that the O_2 solubility increases in the presence of the fluorinated materials (fluorinated silica **6** and Teflon/PVA nanocomposite **8**) compared to that with native PVA and silica. Table 1 also shows an O_2 solubility increase in Teflon/PVA **8** compared to that for fluorinated silica **6**, where a 1.2 ppm increase is shown. O_2 solubility increases in fluorous media has been observed previously in fluorinated artificial blood,[50] ionic liquids,[51] solvents,[52−54] and biological systems.[55,56] As will be evident, the fluorinated solids provide an opportunity to enhance the production of $^1O_2$ due to higher local O_2 concentrations.

Table 1. Oxygen Solubility Enhanced by Fluorinated Materials in Solution[a]

solid	ppm	mM
native silica	14.9 ± 0.4	0.47 ± 0.02
fluorinated silica **6**	16.7 ± 0.4	0.522 ± 0.01
native PVA	14.9 ± 0.03	0.466 ± 0.001
Teflon/PVA **8**	17.9 ± 0.07	0.559 ± 0.003

[a]Pyrex test tubes contained 5.0 mL of O_2-saturated *n*-butanol with 0.58 g of solid at 25 °C. A pO_2 electrode was used to measure the O_2 solubility. After removing the solids from solution, the O_2 solubility returns to 14.9 ppm (0.466 mM).

PEGylated Sensitizer Photorelease from the Fluoropolymers (Figure 6 and Tables 2 and 3). Figure 5 and Table 2 show that the percent of PEGylated sensitizer **13** photoreleased into *n*-butanol was higher for Teflon/PVA **10** than for fluorinated silica **7**. The emergence of sensitizer **13** in *n*-butanol was quantified by monitoring its Q-band absorption by UV−vis. Control experiments show that the red light and O_2 were needed to cause the photorelease of **13**. Control experiments also showed that the ester groups of **7**, **10**, and **13** remained intact under dark reaction conditions. We did not find any evidence for ester bond hydrolysis under the conditions wherein all sensitizer release was due to reaction of $^1O_2$ with the ethene sites. In terms of loading, the quantity of sensitizer loaded onto **7** was greater than that onto **10**. High loading of sensitizer molecules is undesirable, especially when porphyrin sites are within the ~15 Å Förster radius that produces self-quenching for a photothermal[57] rather than a photosensitizer polymer. This led us to examine the number and type of bonds on our fabricated surfaces. Table 3 shows the absolute number of Si−OH, C−OH, C−F, and C−H groups and sensitizer sites in fluorinated silica **7** and Teflon/PVA **10**. The number of O−H bonds for **10** is 4.8-fold greater than that in **7**. For **10** compared to **7**, there are also 1.2-fold more C−F bonds and 1.8-fold less C−H bonds. A driving force in sensitizer adsorption may be the higher number of H-bonding sites in **10** (C−OH 6.2×10^{20}) compared to that in **7** (Si−OH 1.3×10^{20}). There is a greater number of O−H sites on **10** than **7**, which led us to study the adsorptive affinity of sensitizer **13**.

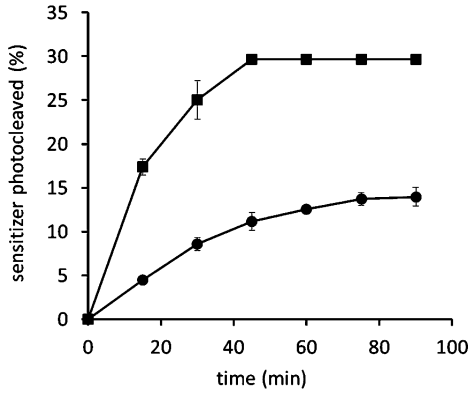

Figure 6. Evolution of sensitizer **13**, which photodeparted away from fluorinated silica **7** (●) and Teflon/PVA **10** (■) into an *n*-butanol solution at 25 °C. Error bars represent the standard deviation obtained from three measurements.

DOI: 10.1021/acs.jpcb.5b00808
J. Phys. Chem. B 2015, 119, 4155−4164

Table 2. Photorelease of Sensitizer on Fluorinated Surfaces[a,b]

solid support	sens loading (nmol)	sens **13** photocleaved (nmol)	% sens photocleaved	sens adsorbed (nmol)	ethene linker bonds broken (nmol)
fluorinated silica **7**	89.4	12.7	68.3	48.4	61.1
Teflon/PVA **10**	21.7	6.5	91.7	13.4	19.9

[a]Red light from a diode laser was used to photocleave the sensitizer. Absorption spectroscopy was used to quantitate the amount of sensitizer **13** in the surrounding *n*-butanol solution. [b]The data show weights for **7** and **10** normalized to 1.0 g.

Table 3. Absolute Number of Bonds or Functional Groups on the Fabricated Surfaces per Gram[a]

solid support	Si−OH	C−OH	C−H	C−F	sens	C−OH/ C−F/sens	Si−OH/C−F/sens
fluorinated silica **7**	1.3×10^{20}		3.5×10^{21}	7.8×10^{21}	5.5×10^{16}		2400:142 000:1
Teflon/PVA **10**		6.2×10^{20}	1.9×10^{21}	9.6×10^{21}	1.3×10^{16}	48 000:75 0000:1	

[a]Fluorinated silica **7** contains pendent nonafluorosilane groups. Teflon/PVA **10** contains repeating $-[CF_2-CF_2]_m-$ and $-[CH_2-CH(OH)]_n-$ units. The penetration depth of sensitizer into solid **7** was 0.08 mm, and that into solid **10** was 1.0 mm.

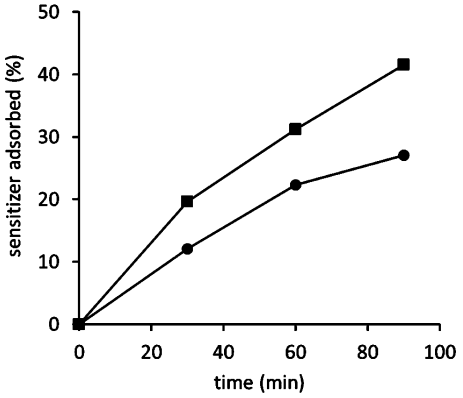

Figure 7. Percent of PEGylated sensitizer **13** adsorbed onto fluorinated surfaces [fluorinated silica **6** (●) and Teflon-PVA **9** (■)] in *n*-butanol. The samples were immersed in *n*-butanol, which contained 10 μM sensitizer **13**, and then the samples were removed at the indicated times.

Testing the Fluorinated Surfaces for Sensitizer Adsorption (Figure 7). We wondered what levels of unwanted adhering of PEG sensitizer **13** would occur with our fluoropolymer supports. Figure 7 shows the amount of sensitizer that adsorbs onto fluoropolymers (here, sensitizerless **6** and **9** were examined) placed in a 10 μM *n*-butanol solution of **13**. The sensitizer's ability to adsorb to the surfaces was increased for **9** compared to that for **6**. This can be understood by the tendency of PEGylated compounds to adhere to surfaces with O−H groups. This result is similar to our recent work,[48] where a pheophorbide sensitizer increased its adsorptive affinity for silica with higher quantities of O−H groups. The number of O−H bonds was important to tabulate because they can serve as adsorption sites. Next, we examined the physical quenching of $^1O_2$ by the fluoropolymers, where less would be better.

Lifetime Measurements (Table 4). Table 4 shows that the total rate constants (k_T) of $^1O_2$ decreased in the presence of fluorinated silica **6**, Teflon/PVA **8**, and Teflon particles compared to that with native silica. In these experiments, the 1270 nm signal of $^1O_2$ was followed with added quantities of the solid particles in acetone-h_6 at 25 °C. Native silica, **6**, **8**, and Teflon were used because they lacked the sensitizer heads of **7** and **10**, where a constant concentration of rose bengal was used in the heterogeneous mixtures. Teflon, **6**, and **8** contain a high number of C−F oscillators, which do not efficiently physically quench $^1O_2$ compared to that by C−H or O−H oscillators due to electronic to vibronic overlap.[58,59] Consistent with this notion, for native silica, the k_T value increased by 2−3-fold because of the greater numbers of O−H bonds. The poor R^2 values in entries 3 and 4 (Table 4) are not a cause for concern where Teflon/PVA **8** and Teflon were ground to flakes that were larger and harder to stir as a slurry than the silica particles. Clearly, the data show success in using fluorinated surfaces due to their reduced physical quenching of $^1O_2$. The low k_T values we observe are encouraging since less wasted $^1O_2$ by the fluorinated surface is vital to its success for drug photorelease, as is described next.

Table 4. Rates of Reaction with Singlet Oxygen by Native Silica, Fluorinated Silica 6, Teflon/PVA 8, and Teflon in Acetone[a]

entry	sample	k_T (L g^{-1} s^{-1})	R^2
1	native silica[a]	71 ± 6	0.90
2	fluorinated silica **6**[a]	27 ± 3	0.99
3	Teflon/PVA **8**	29 ± 9	0.84
4	Teflon	10 ± 8	0.60

[a]Heterogeneous mixture of particles (75−150 μm sized silica and ~300−400 μm sized Teflon) in acetone-h_6 at 25 °C. Average of 2−3 experiments.

Mechanism of Sensitizer Photorelease from the Teflon-Like Surfaces (Figure 8). A proposed mechanistic explanation of the results is as follows:

(i). O_2 Solubility. There is enhanced O_2 solubility with our fluoropolymers compared to that in nonfluorinated media, so more $^1O_2$ can be generated. Fluoropolymer surface topology likely relates to O_2 solubility increases based on previous NMR studies,[60] where shapes of perfluoro sites and the existence of cavities in the liquid phase dominate over any direct interactions of O_2 with the fluorine atoms, such as charge-transfer interactions.

(ii). Steric Effects. Singlet oxygen is generated by surfaces **7** and **10**, mainly from surface triplet sensitizer* quenching by O_2 that leads to a dioxetane. We know that the dioxetane is not stable[61,62] and spontaneously breaks apart at room temperature, so the covalent bond between the sensitizer and the surface is lost. As yet, increased kinetic persistence of dioxetanes through sterics, as has been noted in adamantaneadamantylidene dioxetane which is stable at room temperature,[63] cannot be attributed to our fluoropolymers. But, compare parts A and B of Figure 8, where the fluorine groups are oriented differently. Because fluorinated silica **7** consists of branched fluorosilane (high aspect ratio) groups, it is more subject to dynamical motion,[64] whereas Teflon/PVA **10** consists of continuous end-on carbon−fluorine chains in which Teflon $-[CF_2-CF_2]_m-$ may also coil into a helix due to repulsion between vicinal

DOI: 10.1021/acs.jpcb.5b00808
J. Phys. Chem. B 2015, 119, 4155−4164

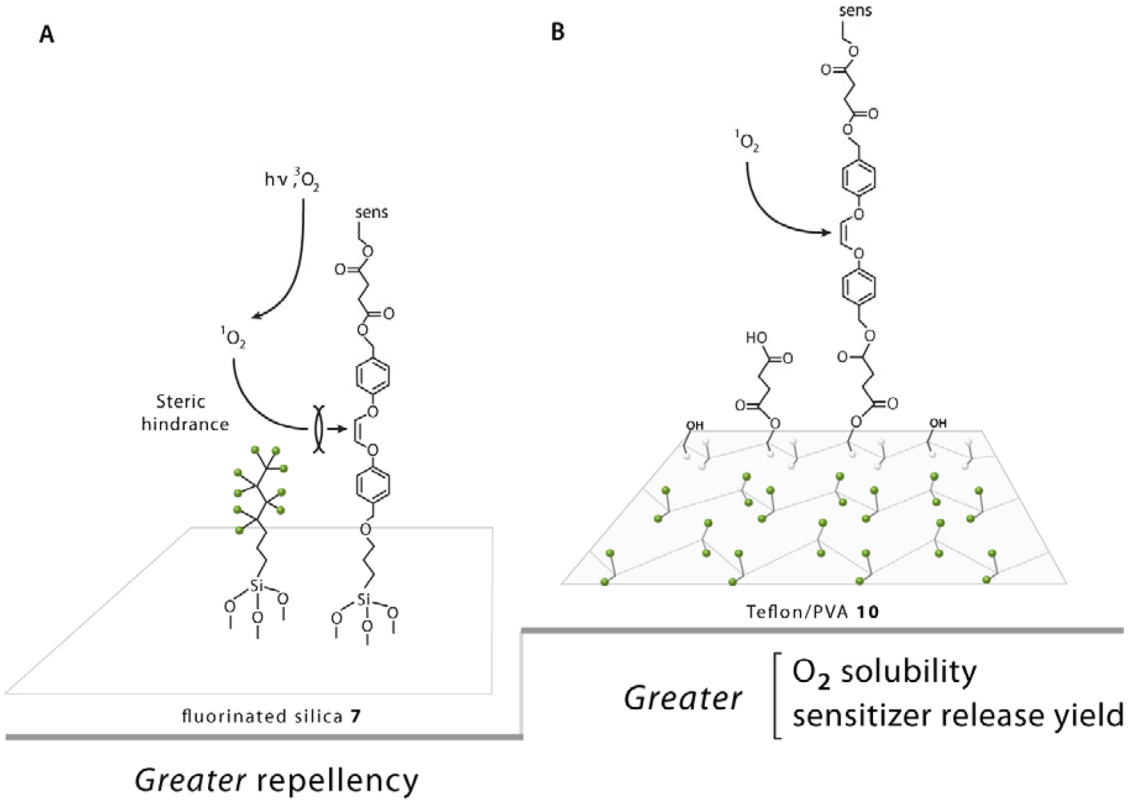

Figure 8. Mechanism of photorelease of sensitizer drug bound to (A) fluorinated silica **7** and (B) Teflon/PVA **10**. The green spheres are fluorine atoms.

fluorine atoms.[65] The importance of steric interactions of the fluorosilane is consistent with our observation of a reduced photocleavage efficiency in **7** compared to that in **10**, but this is confounded by factors such as repelling and quenching (described below). However, it seems obvious that crowding by branched fluorosilanes can prevent $^1O_2$ accessibility to the ethene site. Indeed, dioxetane experiments come to mind that can probe mechanical,[66] cage and chemiluminescence,[67−69] and dynamical features of the ∼1.2 nm length fluorosilane, i.e., nanoheterogeneity, of **7** and **10**, but these are beyond the scope of the present study.

(iii). Resistance to Adsorption. After the ethene is photooxidized and broken, there is a partition between surface release and adsorption channels. The shuttling[70] or mobility of the sensitizer on the surface prior to departure was not scrutinized with our fluoropolymers. However, the small decrease in the adsorptive affinity of **13** for **10** compared to that for **7** is attributed to the higher number of surface O−H groups in **10** relative to **7**. However, does the adsorptive affinity interfere with further ethene photooxidation? Tying up some of sensitizer **13** in an adsorbed state means that autocatalytic-assisted release kinetics are unavailable, unlike that for more repellent hydrophobic sensitizers.[71]

(iv). Reactive Ethene Sites: Inert Support. For our fluoropolymers **7** and **10**, the ethene sites are photooxidized. The data point to fluorinated media and an increase in τ_Δ due to inefficient radiationless deactivation of $^1O_2$ by C−F bonds compared to O−H and C−H bonds.[72−74] Unlike polyfunctionalized compounds or proteins,[75,76] the reaction center for **7** and **10** is the ethene site. Other than the ethene site, the surfaces do not chemically react with $^1O_2$, as would be expected for Teflon-like materials that are known to resist oxidation.[77−80] We find the PEG groups of **7** and **10** were not susceptible to photooxidation. This is not the case for oxygen radicals, e.g., via autoxidation, where PEG hydroperoxides can form and degrade.[81]

In summary, we find that the presence of C−F bonds in these materials leads to efficient photocleavage of the PEGylated sensitizer. Teflon/PVA **10** provides a slight advantage with respect to the sensitizer photorelease application compared to that with fluorinated silica **7**.

■ CONCLUSIONS

We have developed two fluoropolymers and examined their ability to photorelease a PEGylated sensitizer drug. The presence of C−F bonds in the polymers is beneficial for high O_2 solubility, repelling action, and low physical quenching of $^1O_2$. Designing photoactive repellent surfaces so that drugs are released rather than retained is largely an empirical endeavor and remains a challenge. However, opportunities exist by integrating methodologies from the photosciences to engineering to address the problem.

Future Directions. We have synthesized surfaces that are Teflon-like, so a PEGylated sensitizer drug that is otherwise quite sticky can be photoreleased into the surrounding solution; however, further advancements could be made. The fluoropolymers could be shaped into device tips to discharge controlled sensitizer and $^1O_2$ quantities for tissue repair[82,83] or pointsource photodynamic therapy[84] in vivo. The fluorinated materials provide intriguing possibilities for generating new types of device tips for manual precision in singlet oxygen delivery. Next, we will turn to in vivo experiments to examine the fluoropolymers' functional capacity in a mouse tumor model for sensitizer delivery and tumor killing but not biofouling.

DOI: 10.1021/acs.jpcb.5b00808
J. Phys. Chem. B 2015, 119, 4155−4164

■ ASSOCIATED CONTENT

Supporting Information

Absorption, FT-IR, HRMS, and ^{1}H and ^{13}C NMR spectra for **1**−**5**. Absorption and FT-IR spectra of solids **7** and **10**. This material is available free of charge via the Internet at http://pubs.acs.org.

■ AUTHOR INFORMATION

Corresponding Author

*E-mail: agreer@brooklyn.cuny.edu.

Notes

The authors declare no competing financial interest.

■ ACKNOWLEDGMENTS

G.G, M.M., A.A.G., I.A., and A.G. acknowledge support from the National Institute of General Medical Sciences (NIH SC1GM093830). K.C. and T.M.B. acknowledge support from the NIH (P01 CA087971). A.G. acknowledges support from the George and Beatrice Schwartzman Professorship in Chemistry at Brooklyn College. We thank Leda Lee for the graphic arts work.

■ REFERENCES

(1) Klán, P.; Šolomek, T.; Bochet, C. G.; Blanc, A.; Givens, R.; Rubina, M.; Popik, V.; Kostikov, A.; Wirz, J. Photoremovable Protecting Groups in Chemistry and Biology: Reaction Mechanisms and Efficacy. *Chem. Rev.* **2013**, *113*, 119−191.

(2) Givens, R. S.; Lee, J.-I.; Kotala, M. Mechanistic Overview of Phototriggers and Cage Release. In *Dynamic Studies in Biology: Phototriggers, Photoswitches, and Caged Biomolecules*; Goeldner, M., Givens, R., Eds.; Wiley and Sons: Weinheim, Germany, 2005; Chapter 2, pp 95−112.

(3) Rolland, J. P.; Van Dam, R. M.; Schorzman, D. A.; Quake, S. R.; DeSimone, J. M. Solvent-Resistant Photocurable "Liquid Teflon" for Microfluidic Device Fabrication. *J. Am. Chem. Soc.* **2004**, *126*, 2322−2323.

(4) Liu, B.; Rolland, J. P.; DeSimone, J. M.; Bard, A. Fabrication of Ultramicroelectrodes Using a "Teflon-Like" Coating Material. *Anal. Chem.* **2005**, *77*, 3013−3017.

(5) Detty, M. R.; Ciriminna, R.; Bright, F.; Pagliaro, M. Environmentally Benign Sol-Gel Antifouling and Foul-Releasing Coatings. *Acc. Chem. Res.* **2014**, *47*, 678−687.

(6) Rissanen, S.; Kumorek, M.; Martinez-Seara, H.; Li, Y.-C.; Jamroz, D.; Bunker, A.; Nowakowaska, M.; Vattulainen, I.; Kepczynski, M.; Rog, T. Effect of PEGylation on Drug Entry into Lipid Bilayer. *J. Phys. Chem. B* **2014**, *118*, 144−151.

(7) Li, Y.-C.; Rissanen, S.; Stepniewski, M.; Cramariuc, O.; Róg, T.; Mirza, S.; Xhaard, H.; Wytrwal, M.; Kepczynski, M.; Bunker, A. Study of Interaction between PEG Carrier and Three Relevant Drug Molecules: Piroxicam, Paclitaxel, and Hematoporphyrin. *J. Phys. Chem. B* **2012**, *116*, 7334−7341.

(8) Chen, W.; Shi, Y.; Feng, H.; Du, M.; Zhang, J. Z.; Hu, J.; Yang, D. Preparation of Copolymer Paclitaxel Covalently Linked via a Disulfide Bond and Its Application on Controlled Drug Delivery. *J. Phys. Chem. B* **2012**, *116*, 9231−9237.

(9) Pai, S. S.; Przybycien, T. M. Protein PEGylation Attenuates Adsorption and Aggregation on a Negatively Charged and Moderately Hydrophobic Polymer Surface. *Langmuir* **2010**, *26*, 18231−18238.

(10) Pai, S. S.; Heinrich, F.; Canady, A. L.; Przybycien, T. M.; Tilton, R. D. Coverage- Dependent Morphology of PEGylated Lysozyme Layers Adsorbed on Silica. *J. Colloid Interface Sci.* **2012**, *370*, 170−175.

(11) Werner, A.; Blaschke, T.; Hasse, H. Microcalorimetric Study of the Adsorption of PEGylated Lysozyme and PEG on a Mildly Hydrophobic Resin: Influence of Ammonium Sulfate. *Langmuir* **2012**, *28*, 11376−11383.

(12) Wang, S.; Gao, R.; Zhou, F.; Selke, M. Nanomaterials and Singlet Oxygen Photosensitizers: Potential Applications in Photodynamic Therapy. *J. Mater. Chem.* **2004**, *14*, 487−493.

(13) Li, W.; Lu, W.; Fan, Z.; Zhu, X.; Reed, A.; Newton, B.; Zhang, Y.; Courtney, S.; Tiyyagura, P. T.; Ratcliff, R. R.; et al. Enhanced Photodynamic Selectivity of Nano-Silica-Attached Porphyrins against Breast Cancer Cells. *J. Mater. Chem.* **2012**, *22*, 12701−12708.

(14) Arzoumanian, E.; Ronzani, F.; Trivella, A.; Oliveros, E.; Sarakha, M.; Richard, C.; Blanc, S.; Pigot, T.; Lacombe, S. Transparent Organosilica Photocatalysts Activated by Visible Light: Photophysical and Oxidative Properties at the Gas−Solid Interface. *ACS Appl. Mater. Interfaces* **2014**, *6*, 275−288.

(15) Ikeda, Y.; Nagasaki, Y. PEGylation Technology in Nanomedicine. *Adv. Polym. Sci.* **2012**, *247*, 115−140.

(16) Chessick, J. H.; Healey, F. H.; Zettlemoyer, A. C. Adsorption and Heat of Wetting Studies of Teflon. *J. Phys. Chem.* **1956**, *60*, 1345−1347.

(17) Šebej, P.; Wintner, J.; Müller, P.; Slanina, T.; Anshori, J. A.; Antony, L. A. P.; Klán, P.; Wirz, J. Fluorescein Analogues as Photoremovable Protecting Groups Absorbing at ∼520 nm. *J. Org. Chem.* **2013**, *78*, 1833−1843.

(18) Doane, T.; Cheng, Y.; Sodhi, N.; Burda, C. NIR Photocleavage of the Si−C Bond in Axial Si-Phthalocyanines. *J. Phys. Chem. A* **2014**, *118*, 10587−10595.

(19) Borak, J. B.; Falvey, D. E. Ketocoumarin Dyes as Electron Mediators for Visible Light Induced Carboxylate Photorelease. *Photochem. Photobiol. Sci.* **2010**, *9*, 854−860.

(20) Sundararajan, C.; Falvey, D. E. Photorelease of Carboxylic Acids, Amino Acids, and Phosphates from N- Alkylpicolinium Esters Using Photosensitization by High Wavelength Laser Dyes. *J. Am. Chem. Soc.* **2005**, *127*, 8000−8001.

(21) Wang, Z.; Johns, V. K.; Liao, Y. Controlled Release of Fragrant Molecules with Visible Light. *Chem.—Eur. J.* **2014**, *20*, 14637−14640.

(22) Sgambellone, M. A.; David, A.; Garner, R. N.; Dunbar, K. R.; Turro, C. Cellular Toxicity Induced by the Photorelease of a Caged Bioactive Molecule: Design of a Potential Dual-Action Ru(II) Complex. *J. Am. Chem. Soc.* **2013**, *135*, 11274−11282.

(23) Jana, A.; Ikbal, M.; Singh, N. D. P. Perylen-3-ylmethyl: Fluorescent Photoremovable Protecting Group (FPRPG) for Carboxylic Acids and Alcohols. *Tetrahedron* **2012**, *68*, 1128−1136.

(24) Lin, Q.; Bao, C.; Yang, Y.; Liang, Q.; Zhang, D.; Cheng, S.; Zhu, L. Highly Discriminating Photorelease of Anticancer Drugs Based on Hypoxia Activatable Phototrigger Conjugated Chitosan Nanoparticles. *Adv. Mater.* **2013**, *25*, 1981−1986.

(25) Shanmugam, V.; Selvakumar, S.; Yeh, C.-S. Near-Infrared Light-Responsive Nanomaterials in Cancer Therapeutics. *Chem. Soc. Rev.* **2014**, *43*, 6254−6287.

(26) Carling, C.-J.; Viger, M. L.; Nguyen Huu, V. A.; Garcia, A. V.; Almutairi, A. In Vivo Visible Light-Triggered Drug Release From an Implanted Depot. *Chem. Sci.* **2015**, *6*, 335−341.

(27) Zamadar, M.; Ghosh, G.; Mahendran, A.; Minnis, M.; Kruft, B. I.; Ghogare, A.; Aebisher, D.; Greer, A. Photosensitizer Drug Delivery via an Optical Fiber. *J. Am. Chem. Soc.* **2011**, *133*, 7882−7891.

(28) Mahendran, A.; Kopkalli, Y.; Ghosh, G.; Ghogare, A.; Minnis, M.; Kruft, B. I.; Zamadar, M.; Aebisher, D.; Davenport, L.; Greer, A. A Hand-Held Fiber-Optic Implement for the Site-Specific Delivery of Photosensitizer and Singlet Oxygen. *Photochem. Photobiol.* **2011**, *87*, 1330−1337.

(29) Nkepang, G.; Bio, M.; Rajaputra, P.; Awuah, S. G.; You, Y. Folate Receptor-Mediated Enhanced and Specific Delivery of Far-Red Light-Activatable Prodrugs of Combretastatin A-4 to FR-Positive Tumor. *Bioconjugate Chem.* **2014**, *25*, 2175−2188.

(30) Bio, M.; Rajaputra, P.; Nkepang, G.; Awuah, S. G.; Hossion, A. M. L.; You, Y. Site-Specific and Far-Red-Light-Activatable Prodrug of Combretastatin A-4 Using Photo-Unclick Chemistry. *J. Med. Chem.* **2013**, *56*, 3936−3942.

(31) Bio, M.; Rajaputra, P.; Nkepang, G.; You, Y. Far-Red Light Activatable, Multifunctional Prodrug for Fluorescence Optical Imaging and Combinational Treatment. *J. Med. Chem.* **2014**, *57*, 3401−3409.

(32) Nkepang, G.; You, Y. Heteroatom-Substituted Dioxetanes and Their Emerging Biomedical Applications. In *The Chemistry of Peroxides*; Greer, A., Liebman, J. F., Eds.; J. Wiley & Sons, Ltd: Chichester, UK, 2014; Vol. 3, pp 683−712.

DOI: 10.1021/acs.jpcb.5b00808
J. Phys. Chem. B 2015, 119, 4155−4164

(33) Flors, C.; Nonell, S. Light and Singlet Oxygen in Plant Defense against Pathogens: Phototoxic Phenalenone Phytoalexins. *Acc. Chem. Res.* **2006**, *39*, 293−300.
(34) Lorente, C.; Arzoumanian, E.; Castaño, C.; Oliveros, E.; Thomas, A. H. A Non-singlet Oxygen Mediated Reaction Photoinduced by Phenalenone, a Universal Reference for Singlet Oxygen Sensitization. *RSC Adv.* **2014**, *4*, 10718−10727.
(35) Hargus, J. A.; Fronczek, F. R.; Vicente, M. G. H.; Smith, K. M. Mono-(L)-aspartylchlorin-e_6. *Photochem. Photobiol.* **2007**, *83*, 1006−1015.
(36) Jinadasa, R. G. W.; Hu, X.; Vicente, M. G. H.; Smith, K. M. Syntheses and Cellular Investigations of 17^3-, 15^2-, and 13^1-Amino Acid Derivatives of Chlorin e_6. *J. Med. Chem.* **2011**, *54*, 7464−7476.
(37) DiMagno, S. G.; Dussault, P. H.; Schultz, J. A. Fluorous Biphasic Singlet Oxygenation with a Perfluoroalkylated Photosensitizer. *J. Am. Chem. Soc.* **1996**, *118*, 5312−5313.
(38) Allémann, E.; Brasseur, N.; Kudrevich, S. V.; La Madeleine, C.; van Lier, J. E. Photodynamic Activities and Biodistribution of Fluorinated Zinc Phthalocyanine in the Murine EMT-6 Tumour Model. *Int. J. Cancer* **1997**, *72*, 289−294.
(39) Yang, S. I.; Seth, J.; Strachan, J.-P.; Gentemann, S.; Kim, D.; Holten, D.; Lindsey, J. S.; Bocian, D. F. Ground and Excited State Electronic Properties of Halogenated Tetraarylporphyrins. Tuning the Building Blocks for Porphyrin-Based Photonic Devices. *J. Porphyrins Phthalocyanines* **1999**, *3*, 117−147.
(40) Gryshuk, A. L.; Chen, Y.; Potter, W.; Ohulchansky, T.; Oseroff, A.; Pandey, R. K. In Vivo Stability and Photodynamic Efficacy of Fluorinated Bacteriopurpurinimides Derived from Bacteriochlorophyll-a. *J. Med. Chem.* **2006**, *49*, 1874−1881.
(41) Ko, Y.-J.; Yun, K.-J.; Kang, M.-S.; Park, J.; Lee, K.-T.; Park, S. B.; Shin, J.-H. Synthesis and in Vitro Photodynamic Activities of Water-Soluble Fluorinated Tetrapyridylporphyrins as Tumor Photosensitizers. *Bioorg. Med. Chem. Lett.* **2007**, *17*, 2789−2794.
(42) Röder, B.; Gorun, S. M.; Gerdes, R.; Litwinski, C. PCT Int. Appl. WO 2011045029 A1 20110421, 2011.
(43) Wilson, S. R.; Yurchenko, M. E.; Schuster, D. I.; Yurchenko, E. N.; Sokolova, O.; Braslavsky, S. E.; Klihm, G. Preparation and Photophysical Studies of a Fluorous Phase-Soluble Fullerene Derivative. *J. Am. Chem. Soc.* **2002**, *124*, 1977−1981.
(44) Lin, N.-J.; Yang, H.-S.; Chang, Y.; Tung, K.-L.; Chen, W.-H.; Cheng, H.-W.; Hsiano, S.-W.; Aimar, P.; Yamamoto, K.; Lai, J.-Y. Surface Self-Assembled PEGylation of Fluoro-Based PVDF Membranes via Hydrophobic- Driven Copolymer Anchoring for Ultra- Stable Biofouling Resistance. *Langmuir* **2013**, *29*, 10183−10193.
(45) Yashiro, B.; Shoda, M.; Tomizawa, Y.; Manaka, T.; Hagiwara, N. Long-Term Results of a Cardiovascular Implantable Electronic Device Wrapped with an Expanded Polytetrafluoroethylene Sheet. *J. Artif. Organs* **2012**, *15*, 244−249.
(46) Pandian, R. P.; Meenakshisundaram, G.; Bratasz, A.; Eteshola, E.; Lee, S. C.; Kuppusamy, P. An Implantable Teflon Chip Holding Lithium Naphthalocyanine Microcrystals for Secure, Safe, and Repeated Measurements of pO_2 in Tissues. *Biomed. Microdevices* **2010**, *12*, 381−387.
(47) Kimani, S.; Ghosh, G.; Ghogare, A.; Rudshteyn, B.; Bartusik, D.; Hasan, T.; Greer, A. Synthesis and Characterization of Mono-, Di-, and Tri-poly(ethylene glycol) Chlorin e_6 Conjugates for the Photokilling of Human Ovarian Cancer Cells. *J. Org. Chem.* **2012**, *77*, 10638−10647.
(48) Bartusik, D.; Aebisher, D.; Ghosh, G.; Minnis, M.; Greer, A. Fluorine End-Capped Optical Fibers for Photosensitizer Release and Singlet Oxygen Production. *J. Org. Chem.* **2012**, *77*, 4557−4565.
(49) Avella, M.; Errico, M. E.; Rimedio, R. PVA−PTFE Nanocomposites: Thermal, Mechanical, and Barrier Properties. *J. Mater. Sci. Lett.* **2004**, *39*, 6133−6136.
(50) Lawson, D. D.; Moacanin, J.; Scherer, K. V., Jr.; Terranova, T. F.; Ingham, J. D. Methods for the Estimation of Vapor Pressures and Oxygen Solubilities of Fluorochemicals for Possible Application in Artificial Blood Formulations. *J. Fluorine Chem.* **1978**, *12*, 221−36.
(51) Pereiro, A. B.; Araujo, J. M. M.; Martinho, S.; Alves, F.; Nunes, S.; Matias, A.; Duarte, C. M. M.; Rebelo, L. P. N.; Marrucho, I. M. Fluorinated Ionic Liquids: Properties and Applications. *ACS Sustainable Chem. Eng.* **2013**, *1*, 427−439.
(52) Fraker, C. A.; Mendez, A. J.; Stabler, C. L. Complementary Methods for the Determination of Dissolved Oxygen Content in Perfluorocarbon Emulsions and Other Solutions. *J. Phys. Chem. B* **2011**, *115*, 10547−10552.
(53) Dias, A. M. A.; Goncalves, C. M. B.; Legido, J. L.; Coutinho, J. A. P.; Marrucho, I. M. Solubility of Oxygen in Substituted Perfluorocarbons. *Fluid Phase Equilib.* **2005**, *238*, 7−12.
(54) Wesseler, E. P.; Iltis, R.; Clark, L. C., Jr. The Solubility of Oxygen in Highly Fluorinated Liquids. *J. Fluorine Chem.* **1977**, *9*, 137−146.
(55) Cosco, D.; Fattal, E.; Fresta, M.; Tsapis, N. Perfluorocarbon-Loaded Micro and Nanosystems for Medical Imaging: A State of the Art. *J. Fluorine Chem.* **2015**, *171*, 18−26.
(56) Wang, J.; Lu, F. Oxygen-Rich Oxidase Enzyme Electrodes for Operation in Oxygen-Free Solutions. *J. Am. Chem. Soc.* **1998**, *120*, 1048−1050.
(57) Carter, K. A.; Shao, S.; Hoopes, M. I.; Luo, D.; Ahsan, B.; Grigoryants, V. M.; Song, W.; Huang, H.; Zhang, G.; Pandey, R. K.; et al. Porphyrin−Phospholipid Liposomes Permeabilized by Near-Infrared Light. *Nat. Commun.* **2014**, *5*, 4546/1−4546/11.
(58) Schmidt, R.; Brauer, H.-D. Radiationless Deactivation of Singlet Oxygen by Solvent Molecules. *J. Am. Chem. Soc.* **1987**, *109*, 6976−6981.
(59) Ogilby, P. R.; Foote, C. S. Chemistry of Singlet Oxygen. 42. Effect of Solvent, Solvent Isotopic Substitution, and Temperature on the Lifetime of Singlet Molecular Oxygen. *J. Am. Chem. Soc.* **1983**, *105*, 3423−3430.
(60) Hamza, M. A.; Serratrice, G.; Stebe, M. J.; Delpuech, J. J. Solute−Solvent Interactions in Perfluorocarbon Solutions of Oxygen. An NMR Study. *J. Am. Chem. Soc.* **1981**, *103*, 3733−3738.
(61) Baumstark, A. L. Thermolysis of Alkyl-1,2-dioxetanes. In *Advances in Oxygenated Processes*; Baumstark, A. L., Ed.; JAI Press: Greenwich, CT, 1988; pp 31−84.
(62) Adam, W.; Trofimov, A. V. Contemporary Trends in Dioxetane Chemistry. In *The Chemistry of Peroxides*; Rappoport, Z., Ed.; Wiley-VCH: New York, 2006; Vol. 2, pp 1171−1209.
(63) Schuster, G. B.; Turro, N. J.; Steinmetzer, H. C.; Schaap, A. P.; Faler, G.; Adam, W. Adamantylideneadamantane-1,2-dioxetane Chemiluminescence and Decomposition Kinetics of an Unusually Stable 1,2-Dioxetane. *J. Am. Chem. Soc.* **1975**, *97*, 7110−7118.
(64) Chen, K.-H.; Lii, J.-H.; Walker, G. A.; Xie, Y.; Schaefer, H. F., III; Allinger, N. L. Molecular Mechanics (MM4) Study of Fluorinated Hydrocarbons. *J. Phys. Chem. A* **2006**, *110*, 7202−7227.
(65) Breiby, D. W.; Sølling, T. I.; Bunk, O.; Nyberg, R. B.; Norrman, K.; Nielsen, M. M. Surprises in Friction-Deposited Films of Poly(tetrafluoroethylene). *Macromolecules* **2005**, *38*, 2383−2390.
(66) Collins, C. G.; Lee, J. M.; Oliver, A. G.; Wiest, O. G.; Smith, B. D. Internal and External Stereoisomers of Squaraine Rotaxane Endoperoxide: Synthesis, Chemical Differences and Structural Revision. *J. Org. Chem.* **2014**, *79*, 1120−1130.
(67) Baader, W. J.; Stevani, C. V.; Bastos, E. L. Chemiluminescence of Organic Peroxides. In *Chemistry of Peroxides*; Rappoport, Z., Ed.; Wiley-VCH: New York, 2006; Vol. 2, pp 1211−1278.
(68) Tanimura, M.; Watanabe, N.; Ijuin, H. K.; Matsumoto, M. Base-Induced Chemiluminescent Decomposition of Bicyclic Dioxetanes Bearing a (Benzothiazol-2-yl)-3-hydroxyphenyl Group: A Radiationless Pathway Leading to Marked Decline of Chemiluminescence Efficiency. *J. Org. Chem.* **2012**, *77*, 4725−4731.
(69) Roda, A.; Di Fusco, M.; Quintavalla, A.; Guardigli, M.; Mirasoli, M.; Lombardo, M.; Trombini, C. Dioxetane-Doped Silica Nanoparticles as Ultrasensitive Reagentless Thermochemiluminescent Labels for Bioanalytics. *Anal. Chem.* **2012**, *84*, 9913−9919.
(70) Kirkpatrick, I.; Worrall, D. R.; Williams, S. L.; Buck, C. J. T.; Meseguer, R. G. Probing the Interplay between Factors Determining Reaction Rates on Silica Gel Using Termolecular Systems. *Photochem. Photobiol. Sci.* **2012**, *11*, 1585−1591.
(71) Bartusik, D.; Minnis, M.; Ghosh, G.; Greer, A. Autocatalytic-Assisted Photorelease of a Sensitizer Drug Bound to a Silica Support. *J. Org. Chem.* **2013**, *78*, 8537−8544.

DOI: 10.1021/acs.jpcb.5b00808
J. Phys. Chem. B 2015, 119, 4155−4164

(72) Pace, A.; Pierro, P.; Buscemi, S.; Vivona, N.; Clennan, E. L. Photooxidations of Alkenes in Fluorinated Constrained Media: Fluoro-Organically Modified NaY as Improved Reactors for Singlet Oxygen "Ene" Reaction. *J. Org. Chem.* **2007**, *72*, 2644−2646.
(73) Hall, J. F. B.; Han, X.; Poliakoff, M.; Bourne, R. A.; George, M. W. Maximizing the Efficiency of Continuous Photooxidation with Singlet Oxygen in Supercritical CO_2 by Use of Fluorous Biphasic Catalysis. *Chem. Commun.* **2012**, *48*, 3073−3075.
(74) Schmidt, R. Influence of Heavy Atoms on the Deactivation of Singlet Oxygen ($^1\Delta_g$) in Solution. *J. Am. Chem. Soc.* **1989**, *111*, 6983−6987.
(75) Lemp, E.; Zanocco, A. L.; Lissi, E. A. Linear Free Energy Relationship Analysis of Solvent Effects on Singlet Oxygen Reactions. *Photochem. Photobiol. Sci.* **2012**, *11*, 1585−1591.
(76) Chin, K. K.; Trevithick-Sutton, C. C.; McCallum, J.; Jockusch, S.; Turro, N. J.; Scaiano, J. C.; Foote, C. S.; Garcia-Garibay, M. A. Quantitative Determination of Singlet Oxygen Generated by Excited State Aromatic Amino Acids, Proteins, and Immunoglobulins. *J. Am. Chem. Soc.* **2008**, *130*, 6912−6913.
(77) Hoflund, G. B.; Everett, M. L. Chemical Alteration of Poly(tetrafluoroethylene) TFE Teflon Induced by Exposure to Electrons and Inert-Gas Ions. *J. Phys. Chem. B* **2004**, *108*, 16676−16683.
(78) Bernini, R.; Cacchi, S.; Fabrizi, G.; Forte, G.; Niembro, S.; Petrucci, F.; Pleixats, R.; Prastaro, A.; Shafir, A.; Vallribera, A. Perfluoro-Tagged Gold Nanoparticles Immobilized on Fluorous Silica Gel: A Reusable Catalyst for the Benign Oxidation and Oxidative Esterification of Alcohols. *ChemSusChem* **2009**, *2*, 1036−1040.
(79) De Vietro, N.; Annese, C.; D'Accolti, L.; Fanelli, F.; Fusco, C.; Fracassi, F. New Synthetic Approach to Oxidation Organocatalysts Supported on Merrifield Resin Using Plasma-Enhanced Chemical Vapor Deposition. *Appl. Catal., A: General.* **2014**, *470*, 132−139.
(80) Rahnamoun, A.; van Duin, A. C. T. Reactive Molecular Dynamics Simulation on the Disintegration of Kapton, POSS Polyimide, Amorphous Silica, and Teflon During Atomic Oxygen Impact Using the Reaxff Reactive Force-Field Method. *J. Phys. Chem. A* **2014**, *118*, 2780−2787.
(81) Hamburger, R.; Azaz, E.; Donbrow, M. Autoxidation of Polyoxyethylenic Non-ionic Surfactants and of Polyethylene Glycols. *Pharm. Acta Helv.* **1975**, *50*, 10−17.
(82) Johnson, T. S.; O'Neill, A. C.; Motarjem, P. M.; Amann, C.; Nguyen, T.; Randolph, M. A.; Winograd, J. M.; Kochevar, I. E.; Redmond, R. W. Photochemical Tissue Bonding: A Promising Technique for Peripheral Nerve Repair. *J. Surg. Res.* **2007**, *143*, 224−229.
(83) Yao, M.; Gu, C.; Doyle, F. J., Jr.; Zhu, H.; Redmond, R. W.; Kochevar, I. E. Why Is Rose Bengal More Phototoxic to Fibroblasts in Vitro than in Vivo? *Photochem. Photobiol.* **2014**, *90*, 297−305.
(84) Ghogare, A. A.; Rizvi, I.; Hasan, T.; Greer, A. Pointsource Delivery of a Photosensitizer Drug and Singlet Oxygen: Eradication of Glioma Cells in Vitro. *Photochem. Photobiol.* **2014**, *90*, 1119−1125.

DOI: 10.1021/acs.jpcb.5b00808
J. Phys. Chem. B 2015, 119, 4155−4164